The influence of cochlear shape on low-frequency hearing

Daphne Manoussaki*†, Richard S. Chadwick‡§, Darlene R. Ketten‡¶‖, Julie Arruda‖**, Emilios K. Dimitriadis††, and Jen T. O'Malley**

*Department of Mathematics, Vanderbilt University, Nashville, TN 37240; †Department of Sciences, Technical University of Crete, Hania, Greece 73100; ‡Auditory Mechanics Section, National Institute on Deafness and Other Communication Disorders, and ††Laboratory of Bioengineering and Physical Science, National Institute of Biomedical Imaging and Bioengineering, National Institutes of Health, Bethesda, MD 20892; ¶Department of Otology and Laryngology, Harvard Medical School, Boston, MA 02114; ‖Woods Hole Oceanographic Institution, Woods Hole, MA 02543; and **Massachusetts Ear and Eye Infirmary, Boston, MA 02114

Edited by Jon H. Kaas, Vanderbilt University, Nashville, TN, and approved February 13, 2008 (received for review October 22, 2007)

The conventional theory about the snail shell shape of the mammalian cochlea is that it evolved essentially and perhaps solely to conserve space inside the skull. Recently, a theory proposed that the spiral's graded curvature enhances the cochlea's mechanical response to low frequencies. This article provides a multispecies analysis of cochlear shape to test this theory and demonstrates that the ratio of the radii of curvature from the outermost and innermost turns of the cochlear spiral is a significant cochlear feature that correlates strongly with low-frequency hearing limits. The ratio, which is a measure of curvature gradient, is a reflection of the ability of cochlear curvature to focus acoustic energy at the outer wall of the cochlear canal as the wave propagates toward the apex of the cochlea.

inner ear | function | mammalian evolution | spiral

It is often thought that mammalian cochleae are coiled to pack a longer organ into a small space inside the skull and that the cochlear coil increases the efficiency of blood and nerve supply through a central shaft (1). Although these spatial advantages of a coiled cochlea have been generally accepted, understanding the effect of shape on hearing itself has been a challenge.

Cochlear coiling is absent in reptiles, birds, and monotreme mammals, and it appears to have originated in the marsupial and placental mammal lines (2). Coiling allowed the cochlea to become longer, increasing the potential octave range, whereas uncoiled cochleae have been associated with relatively limited hearing ranges. Earlier studies suggested that the evolution of coiling enhanced high-frequency hearing (3). This suggestion, however, is not wholly satisfactory for several reasons. Above all, increased hearing ranges extended both high-frequency and low-frequency (LF) hearing abilities in mammals compared with birds and reptiles and improved sensitivities compared with even LF specialist fishes (4). Further, the highest-frequency waves are resolved near the base (entrance) before they propagate far enough into the spiral to "feel" the cochlear curvature; it is the lowest-frequency waves that propagate along the cochlea's coils.

Earlier work on land mammal ear anatomy (5) found a strong correlation between the LF hearing limit of each species and the product of basilar membrane length and number of spiral turns, but did not adduce a mechanistic explanation for this relationship. Other data suggested also that longitudinal curvature of the cochlear duct generates radial fluid pressure gradients (6) and enhances radial movement of hair cells (1, 7).

Recently, a new theory proposed that the cochlea's graded curvature actually enhances LF hearing (8), similar to a whispering gallery in which sounds cling to the concave surface of the lateral wall (9). The cochlear spiral shape redistributes wave energy toward the outer wall, particularly along its innermost, tightest, apical turn, and thereby enhances sensitivity to lower-frequency sounds.

In this article, we test this theory morphometrically. We use the ratio of the radius of curvature at the base of the spiral to the radius of curvature at the apex as a single, simple measure of curvature change (and thus, energy redistribution), and show that it is a robust correlate of LF hearing limits for both land and aquatic mammals. Contrary to the existing literature that has suggested that material properties and geometry local to the LF region control the LF limit (10, 11), we suggest that this measure of curvature change of the entire cochlea affects the LF limit.

To understand the effect of change of curvature, one must look at how the cochlea functions. Incoming sounds are transmitted to cochlear fluids by the eardrum (tympanic membrane) and three small articulated bones (the ossicles) that connect the tympanic membrane to a second membrane (oval window) sealing one of the three chambers of the fluid-filled cochlear spiral. The resulting pressure oscillations in the cochlear fluids deflect the basilar membrane (BM), a membranous partition that forms one boundary of the central chamber (scala media) and spans the length of the spiral cochlea. This deflection propagates along the BM from the oval window toward the spiral apex as a transverse traveling wave with a time-varying peak displacement envelope. At high frequencies, the amplitude of the traveling wave is maximized near the cochlear base where the BM is stiffest. The traveling wave is effectively terminated shortly thereafter. At LFs, the wave travels the full length of the spiral and achieves its maximum amplitude near the spiral's apex where the BM is more compliant (12). The mechanical properties of the BM as well as the energy density traveling along the cochlea control the characteristics of motion of the traveling wave.

However, both the peak amplitude of the traveling wave and the radial profile of the transverse wave are important. Neurosensory hair cells seated atop the BM are stimulated by radial shear forces. Hair cells are therefore responsive to radial variations in BM motion. We thus suggest that the spiral shape affects strongly these radial motion variations, and by doing so, it also affects hair cell stimulation and hearing.

Calculation of Sound Energy Focusing at the Apex

The radial profile of the BM wave is a result of the wave energy distribution across the cochlear channel. As wave energy propagates along the spiral, energy propagation paths glance off a wall with increasing curvature, and thus progressively focus toward the outer wall (8). The energy propagation pathways are

Author contributions: D.M. and R.S.C. designed research; D.M., R.S.C., D.R.K., J.A., and J.T.O. performed research; D.M., R.S.C., and E.K.D. contributed new reagents/analytic tools; D.M., R.S.C., D.R.K., J.A., and J.T.O. analyzed data; and D.M., R.S.C., and D.R.K. wrote the paper.

The authors declare no conflict of interest.

This article is a PNAS Direct Submission.

Freely available online through the PNAS open access option.

§To whom correspondence should be addressed. E-mail: chadwick@helix.nih.gov.

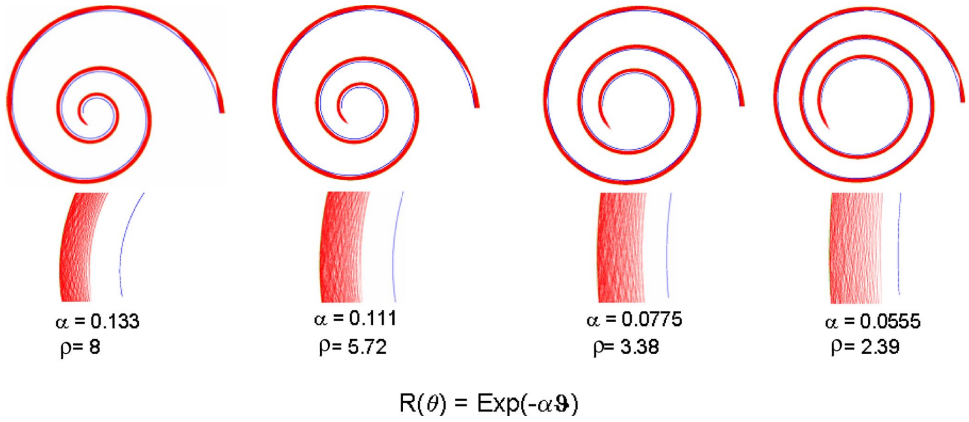

Fig. 1. Focusing of rays by spirals. A uniform distribution of 200 rays (red) entering and filling a spiral duct (walls in blue) at the largest radius is increasingly focused toward the outer wall as the rays progress toward the apex (spiral center). The effect increases with the parameter α, which controls the rate of decrease of radius in the exponential spirals described by the formula given in the figure. *Insets* shown below each spiral, in an expanded scale, indicate the radial gradient of ray or energy density at the apex. These distributions should be compared with a uniform distribution of rays entering at the largest radius to see the energy density focusing effect of the spiral walls.

likened to sound propagation in a whispering gallery, only the cochlear spiral, because of this focusing, is more effective.

Regardless of the mechanism for the encoding of the lower frequencies (phase locking or, as for higher frequencies, amplitude-place mapping), changing energy density distribution along the radial direction would change the radial profile of the vibration of the different cochlear structures (7), affecting LF hearing. In particular, energy density focusing at the outer wall increases the dynamic displacement $\eta = \eta(r, \theta)$ of the BM normal to the resting position, and creates an effective radial tilt T in the BM motion that is equal to the difference in displacement $\Delta\eta$ between inner and outer walls divided by BM width w_{bm}:

$$T = \frac{\Delta\eta}{w_{\mathrm{bm}}} \propto \frac{w_{\mathrm{bm}}^2}{\lambda^{7/2} R_m}\left(1 + \frac{w_{\mathrm{bm}}^2}{10\ R_m^2}\right), \qquad [1]$$

where R_m is the radial position of the BM midline and λ is the wavelength of the associated longitudinal wave (8). R_m and λ decrease from base to apex, w_{bm} increases, and so the tilt in the BM motion increases from base to apex, with relative change in the dynamic BM tilt equal to

$$\frac{T_{\mathrm{apex}} - T_{\mathrm{base}}}{T_{\mathrm{base}}} \approx \frac{\Lambda^{7/2}\rho}{W^2}\left(1 + \frac{w_{\mathrm{bm}}^2}{10\ R_m^2}\right)_{\mathrm{apex}} - 1, \qquad [2]$$

where $W = w_{\mathrm{base}}/w_{\mathrm{apex}}$, $\Lambda = \lambda_{\mathrm{base}}/\lambda_{\mathrm{apex}}$, and $\rho = R_{\mathrm{base}}/R_{\mathrm{apex}}$. Only part of the wavelength contribution, Λ^2, to dynamic BM tilt is a result of changes in the radial distribution of energy density. The remainder, $\Lambda^{3/2}$, is due to amplification of the wave in a cochlea with graded BM compliance (ref. 8, equation 23) and appears also in analyses of straight cochlear mechanics. Nevertheless, tilting of the BM is augmented by shorter waves that help to reduce longitudinal fluid coupling (16). Given that energy density at an angular position θ along the spiral is the product of pressure times velocity along the spiral $E(\theta) = PV_\theta$ (8), we calculate the difference in energy density between the outer and inner walls of the cochlear duct at an angular position θ along the spiral:

$$\Delta E(\theta) = E_{\mathrm{outer}} - E_{\mathrm{inner}} \approx \frac{\mathrm{constant}}{R_m(\theta)}\left(1 + \frac{w_{bm}(\theta)^2}{6\ R_m(\theta)^2}\right). \qquad [3]$$

This result assumes that waves propagate to the LF region. An estimate for the energy focusing at a position θ along the spiral can thus be given by the ratio of energy difference at angular position θ to the energy difference at the cochlea base:

$$\frac{\Delta E(\theta)}{\Delta E_{\mathrm{base}}} \approx \frac{R_{\mathrm{base}}}{R_m(\theta)}\left(1 + \frac{w_{\mathrm{bm}}(\theta)^2}{6\ R_m(\theta)^2}\right). \qquad [4]$$

The results in Eqs. **3** and **4**, to leading order, do not depend on the wavelength. According to Eq. **4**, energy focusing at an angular position θ along the spiral is inversely proportional to the ratio of the corresponding radii of curvature. The ratio, and thus energy focusing, becomes greatest at the apex, where the ratio of the radius of curvature at the base to radius of curvature at the apex is greatest, and where low frequencies are resolved:

$$\frac{\Delta E_{\mathrm{apex}}}{\Delta E_{\mathrm{base}}} \approx \rho\left(1 + \frac{w_{\mathrm{bm}}^2}{6\ R_m^2}\right)_{\mathrm{apex}}, \qquad [5]$$

where $\rho = R_{\mathrm{base}}/R_{\mathrm{apex}}$. Note that the terms in parentheses need to be evaluated only at the apex, because similar terms at the base are close to unity. The widening of the BM toward the apex augments the focusing due to curvature, but the effect does not contribute as much variation across species as does the radii ratio. The approximation above is a conservative estimate of energy focusing, because higher-order terms have all positive signs. The effect of energy focusing at the apex is also demonstrated by ray tracing in Fig. 1, which shows how spirals with a larger ratio of outer to inner radii focus a uniform distribution of incoming rays better. In the cochlea, graded stiffness would make the effect potentially larger. To probe the potential effect of energy density increase in LF hearing, we consider the radii ratio ρ across a range of mammalian species. We hypothesize that the larger this ratio, the better the LF sensitivity. Plotting behavioral LF hearing limits against their respective radii ratio demonstrates a robust correlation in support of our hypothesis.

Results and Discussion

Behavioral audiograms and morphometric data are listed in Table 1. The data are presented graphically in Figs. 2 and 3. All species included in the present dataset have generalist ears and thus typical mammalian hearing abilities that span seven to nine octaves and extend well into high frequencies and LFs. We note, however, that specialist cochleae in both land and marine species, such as the ears of the mole rat, horseshoe bat, mous-

Table 1. Morphometric and frequency data for mammals

Common name (*Species*)	Frequency and morphometric data: Symbol in Figs. 2 and 3	60-dB LF limit, Hz	Radii ratio	Radii data source*	BM length *L*, mm	Turns, *n*	BM apex width, thickness, μm	Refs.
Bottlenose dolphin (*Tursiops truncatus*)	bd	150	4.3	CT, hist	38.9	2.25	380, 5	14, 21
Cat (*Felix catus*)	ca	55	6.2	CT, hist and lit	25.8	3	420, 5	5, 13, 14, 22
Chinchilla (*Chinchilla lanigera*)	ch	52	6.4	CT, hist	18.5	3	310, 6	5, 13, 14, 24
Cow (*Bos taurus*)	cw	23	8.9	lit	38	3.5	–	1, 5, 13, 14, 23
Elephant (*Elephas maximus*)	e	17	8.8	CT, lit	60	2.25	–	1, 5, 13, 14, 25
Gerbil (*Meriones unguiculatis*)	gb	56	6.8	CT, lit	12.1	3.25	250, –	1, 5, 13, 26
Guinea pig (*Cavia porcellus*)	gp	47	7.2	CT, lit	18.5	4	245, 2	5, 13, 27
Human (*Homo sapiens*)	h	31	8.2	CT, lit	33.5	2.5	504, 2	1, 5, 28
Mouse (*Mus musculus*)			1.7	CT, hist and lit	6.8	2	160, 1	1, 5
NMRI strains	ms1	900						29, 30
Other strains	ms2	2,000						31
Rabbit (*Oryctolagus cuniculus*)	rb	96	–	lit	15.2	2.25	–	5, 13, 32
Rat (*Rattus norvegicus*)			3.1	lit	10.7	2.2	250, 2	1, 5, 13
Albino rat	ra1	390						33
Hooded rat	ra2	530						34
Sea lion (*Zalophus californianus*)	sl	180 (air) 200 (water)	5.2	CT, hist	54.3	1.75	–	21, 35
Squirrel monkey (*Saimiri sciureus*)	sm	100	5.5	CT	15.4	2.25	–	5, 36

LF functional hearing limits were established for land mammals as the frequency equivalent to the 60 dB re 20 μPa response threshold in published behavioral audiograms. For the bottlenose dolphin and sea lion in water, the LF limit was determined from the 120 dB re 1 μPa level on behavioral audiograms. The radii ratios were calculated as described in *Methods*. BM apical width and thickness were measured by using histological methods.
*CT, computerized tomography; hist, histology; lit, literature.

tached bat, and harbor porpoise (13, 14), may not fit the generalist correlations. There are insufficient published data available at this time to properly assess these species. Efforts are needed therefore to obtain similar measurements from specialist ears to address these species and to examine issues, such as bimodal distributions of LF or high-frequency hearing, that may also be related to the mechanisms proposed here.

The ratio $\rho = R_{\text{base}}/R_{\text{apex}}$ was linearly correlated with the log of LF hearing limit f ($r = 0.979$, $P < 0.001$) for 13 marine and land mammal species. We rewrite the relationship between ρ and f as

$$f = f_0 \exp[-\beta(\rho - 1)]. \quad \textbf{[6]}$$

For the LF limit of hearing as determined from behavioral audiograms, we calculate that $f_0 = 1{,}507 \pm 241$ Hz and $\beta = 0.578 \pm 0.167$. It is notable that the radii ratio, like functional limits of hearing (13), is independent of animal mass when both land and marine species are considered. For example, the guinea pig has a larger ratio and better LF hearing than the bottlenose dolphin. Our correlation suggests that a hypothetical mammal that has a cochlea with a constant radius of curvature (radii ratio is $\rho = 1$) should have a LF limit of $1{,}507 \pm 241$ Hz at 60 dB (re) 20 μPa. The slope parameter β is 0.578, which implies that just a one-unit increase in radii ratio would result in a relative decrease in LF limit of almost an octave. Because different radii ratios are related to different energy density focusing at the apex, we argue that energy density focusing by use of the spiral geometry is one mechanism used in land and aquatic mammalian cochlea to affect the LF hearing limit.

The characteristic spiral shape has caught the attention of other researchers (see, e.g., refs. 1, 5, and 6), but the curvature gains were first explained in refs. 7 and 8 and in the present work. In ref. 8, the macromechanics of energy focusing because of curvature was considered in a simple model having no tectorial membrane, whereas in ref. 7, the effect of curvature on the hair bundle shear gain in a local cross-section of a complex micromechanical model with a tectorial membrane, but with no energy focusing, was considered. The total gain due to curvature can be estimated as the product of curvature shear gain (7) and gain due to energy focusing from curvature change. The latter can be estimated from Eq. **5** as $\approx 5/3\rho$, where ρ is the radii ratio. The former was calculated as $\approx 18/5$ for the apical cross-section geometry at the low-frequency asymptote(ref. 7; Fig. 3). Thus, the total curvature gain is $\approx 6\rho$. Because ρ varies ≈ 1 order of magnitude over all of the mammalian species, the total curvature gain is ≈ 36 dB, which can explain $\approx 70\%$ of the octave variation in LF hearing limits based on mammalian behavioral audiograms (37). Middle ear characteristics (39) and bone conduction (1) are likely important contributors also to the octave variation in LF limits.

In a previous morphometric study correlating cochlear geometry with behavioral audiograms in different mammals, West (5) found a robust correlation for two hearing parameters and two spiral parameters: (*i*) number of turns vs. octave difference in

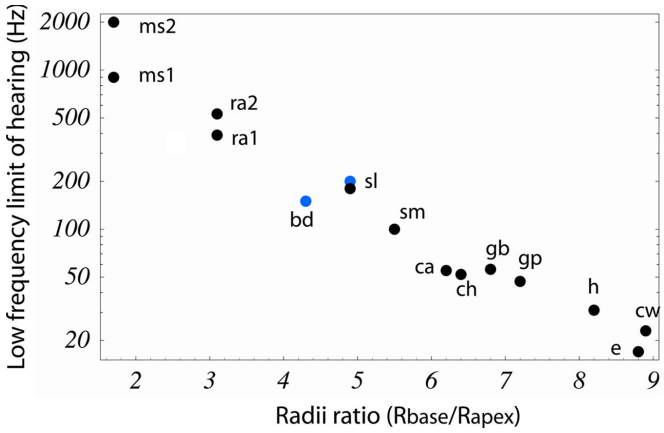

Fig. 2. Land and aquatic mammalian LF hearing relationship with spiral radii ratio. The LF limit of hearing was determined in land (black dots) and marine (blue dots) mammals from behavioral audiograms at 60-dB SPL re 20 μPa_{rms}. Exceptions were the behavioral audiograms in water of the bottlenose dolphin and the sea lion, which were at 120-dB SPL re 1 μPa_{rms} (the sea lion audiogram in air was at 60-dB SPL). Two different mice and rat audiograms are reported because of unresolved disputes in the literature on the LF limits of hearing among strains. Cochlear radii ratios were calculated as the radius of curvature of the basilar membrane midline at the base to that at the apex, according to the technique described in *Methods* (data are summarized in Table 1, including abbreviations). The audiograms are strongly correlated with this dimensionless ratio and indicate that the greater the radii ratio, the lower the LF limit of hearing ($r = 0.979$, $P < 0.001$). This relationship represents a functional anatomical correlate for the energy density focusing theory (8).

BM peak shift LF limit and absolute LF limits, and (*ii*) the product of turn number times BM length vs. LF limit in hertz. A careful examination of the data in West's article (5) shows, however, that the first correlation, turns vs. octave difference in LF limits, contains a sign error in the octave difference for the elephant and therefore does not, in fact, produce a significant correlation (ref. 5, figure 11 and table 2). The second correlation (ref. 5, figure 10) is correctly stated, but no functional explanation to the product of length times turns was given. We have updated this correlation in Fig. 3. Although there is a moderate correlation for the dataset for land mammals, if two marine mammals are added, the correlation is weaker. In fact, BM length alone correlates nearly as well with the LF hearing limit

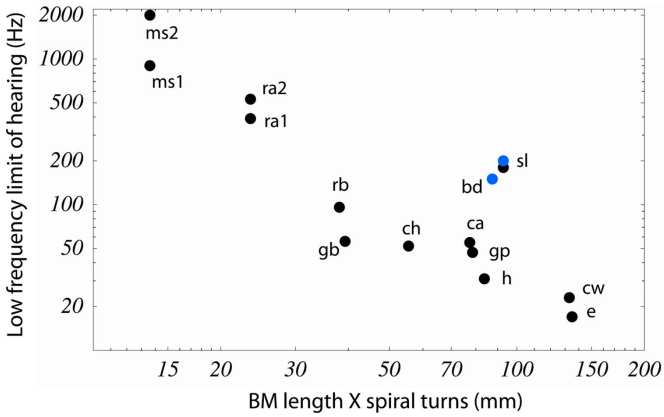

Fig. 3. Mammalian LF hearing relationship to BM length times turns. Behavioral audiogram and cochlear data sources are listed in Table 1. This graph updates a similar data analysis by West (5). The significance level and correlation coefficient for this relationship ($r = 0.827$, $P < 0.001$; $r = 0.901$, $P < 0.001$ land mammals only) is not as strong as that for the relationship of radii ratio and LF limits shown in Fig. 2.

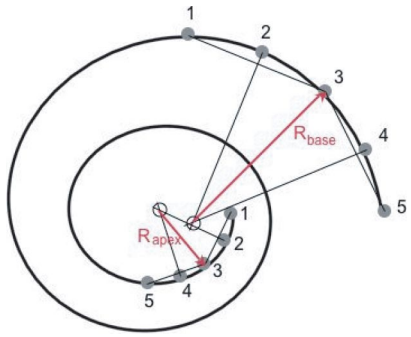

Fig. 4. Schematic of cochlear spiral with five points used to determine radii of curvature. See *Methods* for a description of the construction procedure.

in nonaquatic mammals (ref. 5, figure 10). This is evident because length variations are larger than variations in turn number. Concerning the poor correlation for marine mammals, it should be noted that, although length is the same correlate of body mass for both land and marine mammals, mass does not correlate well with hearing range, and thus LF limits, that would be predicted for a generalist land mammal from length alone (38). We also note that BM apical width, or BM apical width/thickness ratio, given in Table 1, correlates no better than BM length times turns vs. LF hearing limit. This is consistent with the rather small variation across species of BM width on energy focusing in Eq. **5**.

Is cochlear size an important parameter for LF limits? Our calculations indicate that the radii ratio is important, and that the size is not important. This can be seen in two ways, by comparing cochleas of equal length but different ratios or similar ratios but different lengths. Cases for both appear in Table 1. Our correlation supports this result. For example, compare guinea pig, cat, and chinchilla. Guinea pig and chinchilla have similar cochlear lengths but different ratios and LF limits that match the differences in ratios. The cat has a radically different length but a ratio similar to both and a very near LF limit. The body mass of the adult cat is also substantially larger.

One geometrical parameter that, until now, was believed to affect LF hearing is the size of the helicotrema, the pressure relief passageway at the cochlear apex (10, 11). According to this hypothesis, if cochlear fluid flows through the helicotrema without a loss in pressure, then a pressure difference will not act across the adjacent cochlear partition and sound will not be detected. It becomes easier for fluid to flow if the helicotrema area is large, if its length is relatively small, and if the frequency is lower, and, hence, the speed, slower. It then follows that smaller areas allow lower frequencies to be detected better. However, not all measurements concur with this hypothesis. Cat and chinchilla have helicotrema areas 10 times larger than that of the guinea pig and kangaroo rat (10), yet these animals, respectively, have behavioral audiogram LF limits of 55, 52, 47, and 42 Hz at 60-db sound pressure level (SPL). Mice have a smaller helicotrema area than the guinea pig, yet their LF limit is very high, reportedly ranging by strain from 900 to 2,000 Hz. Clearly, the true effect of the helicotrema is not yet fully understood. Perhaps the helicotrema acts to block modulating effects from sounds having a lower frequency than can be detected and thus sharpen responses to audible low frequencies.

At this point, reported effects of the helicotrema are inconsistent and not as strongly correlated with LF limits as radii ratios are. The strongest correlate of LF hearing limits across most species is the dimensionless ratio of basal to apical radii. This relationship (Fig. 2) is robust for virtually all generalist cochleae for which data are available. Any differences by specialists' ears

in LF sensitivity may be because of the different organization of more central auditory processes (15).

There are several implications and applications that result from the theory we present here. First, because the osseous bulla of the cochlea is available in fossils, radii ratios may be determinable, and the LF hearing can be estimated even for mammals that are extinct. Also, because LFs can be localized with less phase ambiguity than high frequencies (17, 40), an increased radii ratio may give a survival advantage for those mammals that use the interaural time difference mechanism to localize sound. We suggest also that the curvature ratio correlation may be useful for studying the evolution of mammalian hearing, similar to studies of the evolution of mammalian balance in which cross-species semicircular canal size and orientation were found to correlate with the degree of locomotor agility (18). Further, interestingly, the radii ratio increases during embryonic development of the cochlea, with the inside of the spiral appearing first, as has been described recently by using mouse explants (19). Genes controlling coiling are also beginning to be identified (20); therefore, experiments on hearing changes with controlled radii ratio variation may become practical.

Methods

Histology. Ears were fixed in 10% neutral buffered formalin and decalcified in 0.27 M EDTA containing 1% formalin. After decalcification, specimens were dehydrated in a graded series of ethanols from 50% through 100%, embedded in celloidin, and hardened. The celloidin-embedded tissue blocks were sectioned at 20 μm, and every 10th section was stained with hematoxylin and eosin and mounted on glass slides for examination.

CT Scans. Fresh, frozen, and formalin-fixed ears were examined by using a Siemens Volume Zoom Helical CT scanner. Scan data were obtained at 0.5- to 1-mm increments with ultra-high bone kernels and imaged at 0.1-mm slice thicknesses in coronal and transaxial planes. Orthogonal projections were obtained by 3D views of the inner ear membranous labyrinth, and associated neural canals were obtained by segmenting x-ray attenuation data for inner ear fluid and bone properties [inner ear views, Woods Hole Oceanographic Institution Computerized Scanning and Imaging Facility (www.whoi.edu/csi)].

Spiral Radii. BM centerlines were estimated from published spirals (1, 21) or from histological sections and CT scans by using both midmodiolar histological sections and midmodiolar CT reformatted sections and reconstructions. To estimate the BM centerline positions, we superimposed the BM path on an orthogonal projection of 3D reconstruction of each inner ear CT scan. Five equally spaced points 1–5 were chosen on each of the first and last quarter turns of the estimated BM paths. The first point was chosen just apical to the cochlear hook. Two chords were constructed between points 1 and 3 and 3 and 5. Perpendiculars to the chords were constructed through points 2 and 4. The intersection of the two perpendiculars determined a local center of curvature from which the radius was determined (Fig. 4).

ACKNOWLEDGMENTS. We thank T. B. Friedman, K. H. Iwasa, B. Shoelson, and N. Gavara for very helpful discussions. This work was supported by National Institutes of Health Intramural Research Program Project Z01-DC000033-10 (R.S.C., E.K.D.), Vanderbilt University and Technical University of Crete (D.M.), and the Office of Naval Research Marine Mammal Program (D.R.K., J.A., and J.T.O.).

1. von Békésy G (1960) *Experiments in Hearing* (McGraw–Hill, New York).
2. Manley GA (2000) Cochlear mechanisms from a phylogenetic viewpoint. *Proc Natl Acad Sci USA* 97:11736–11743.
3. Pye A, Hinchcliffe R (1976) *Scientific Foundations of Otolaryngology*, eds Hinchcliffe R, Harrison D (Year Book Medical Publishers, Chicago), pp 184–202.
4. Popper AN, Ketten DR (2007) *Handbook of the Senses* (Elsevier, Oxford, UK), in press.
5. West CD (1985) The relationship of the spiral turns of the cochlea and the length of the basilar membrane to the range of audible frequencies in ground dwelling mammals. *J Acoust Soc Am* 77:1091–1101.
6. Steele CR, Zais JG (1985) Effect of coiling in a cochlear model. *J Acoust Soc Am* 77:1849–1852.
7. Cai H, Manoussaki D, Chadwick RS (2005) Effects of coiling on the micromechanics of the mammalian cochlea. *J R Soc Interface* 2:341–348.
8. Manoussaki D, Dimitriadis EK, Chadwick RS (2006) Cochleas graded curvature effect on low frequency waves. *Phys Rev Lett* 96:088701.
9. Rayleigh L (1945) *The Theory of Sound* (Dover, New York), Vol 2.
10. Dallos P (1970) Low-frequency auditory characteristics: Species dependence. *J Acoust Soc Am* 48:489–499.
11. Mountain D, *et al.* (2003) *Biophysics of the Cochlea*, ed Gummer AW (World Scientific, London), pp 393–399.
12. von Békésy G (1970) Travelling waves as frequency analysers in the cochlea. *Nature* 225:1207–1209.
13. Echteler SM, Fay RR, Popper AN (1994) *Comparative Hearing: Mammals*, eds Fay RR, Popper AN (Springer, New York), pp 134–171.
14. Ketten DR (2000) *Hearing by Whales and Dolphins*, eds Au WL, *et al.* (Springer, New York), pp 43–108.
15. Schulze H, *et al.* (2002) Superposition of horseshoe-like periodicity and liner tonotopic maps in the auditory cortex of the Mongolian gerbil. *Eur J Neurosci* 15:1077–1084.
16. Lighthill MJ (1978) *Waves in Fluids* (Cambridge Univ Press, Cambridge, UK).
17. Rayleigh L (1907) On our perception of sound direction. *Philos Mag* 13:214–232.
18. Spoor F, Zonneveld F (1998) Comparative review of the human bony labyrinth. *Am J Phys Anthropol* 107:211–251.
19. McKenzie E, Krupin, Kelly MW (2004) Cellular growth and rearrangement during development of the mammalian organ of Corti. *Dev Dyn* 229:802–812.
20. Phippard D, *et al.* (1999) Targeted mutagenesis in the POU-domain gene Brn4/Pou3f4 causes developmental defects in the inner ear. *J Neurosci* 19:5980–5989.
21. Wartzok D, Ketten DR (1999) *Biology of Marine Mammals*, eds Reynolds JE, Rommel SE (Smithsonian Institution Press, Washington, DC), pp 117–175.
22. Heffner RS, Heffner HE (1985) Hearing range of he domestic cat. *Hear Res* 19:85–88.
23. Heffner RS, Heffner HE (1983) Hearing in large mammals-horses (equus-caballus) and cattle (bos-taurus). *Behav Neurosci* 97:299–309.
24. Heffner RS, Heffner HE (1991) Behavioral hearing range of the chinchilla. *Hear Res* 52:13–16.
25. Heffner RS, Heffner HE (1982) Hearing in the elephant (elephas-maximus)-absolute sensitivity, frequency discrimination, and sound localization. *J Comp Physiol Psychol* 96:926–944.
26. Ryan A (1976) Noise-induced threshold shifts in Mongolian gerbil. *J Acoust Soc Am* 59:1222–1226.
27. Heffner RS, Heffner HE, Masterton RB (1971) Behavioral measurement of absolute and frequency-difference thresholds in guinea pig. *J Acoust Soc Am*, 49:1888–1895.
28. International Organization for Standardization (ISO) (1961) Normal equal-loudness level contours. ISO R. 226. (International Organization for Standardization, Geneva).
29. Markl VH, Ehret G (1973) Die horschwelle der maus (*Mus Musculus*). *Z Tierpsychol* 33:274–286.
30. Ehret G (1974) Age-dependent hearing loss in normal hearing mice. *Naturwissenschaften* 61:506–507.
31. Koay G, Harrington I, Heffner RS, Heffner HE (2002) Behavioral audiograms of homozygous med (J)mutant mice with sodium channel deficiency and unaffected controls. *Hear Res* 171:111–118.
32. Heffner H, Masterton R (1980) Hearing in glires—Domestic rabbit, cotton rat, feral house mouse, and kangaroo rat. *J Acoust Soc Am* 68:1584–1599.
33. Kelly JB, Masterton RB (1977) Auditory sensitivity of the albino rat. *J Comp Physiol Psychol* 91:930–936.
34. Heffner HE, Heffner RS, Contos C, Ott T (1994) Audiogram of the hooded Norway rat. *Hear Res* 73:244–248.
35. Kastak D, Schusterman RJ (1998) Low frequency amphibious hearing in pinnipeds: Methods, measurements, noise and ecology. *J Acoust Soc Am* 510:2216–22181.
36. Beecher MD (1974) Pure tone thresholds of the squirrel monkey. *J Acoust Soc Am* 55:196–198.
37. Fay RR (1994) *Comparative Hearing: Mammals*, eds Fay RR, Popper AN (Springer, New York), p 8.
38. Ketten DR, Wartzok D(1990) *Sensory Abilities of Cetaceans: Field and Laboratory Evidence*, Proceedings of NATO ASI Series A 96, eds Thomas J, Kastelein R (Plenum Press, New York), pp 81–105.
39. Rosowski JJ (1992) *The Evolutionary Biology of Hearing*, eds Webster DB, Fay RR, Popper AN (Springer, New York), pp 615–631.
40. Heffner RS, Heffner HE (1992) *The Evolutionary Biology of Hearing*, eds Webster DB, Fay RR, Popper AN (Springer, New York), pp 691–715.